



---

# Design and Control of High Voltage Gain Interleaved Boost Converter for Fuel Cell Based Electric Vehicle Applications

---

S. Madan Gopal<sup>1\*</sup>, K. Meenendranath Reddy<sup>2</sup>

<sup>1\*</sup>PG Student, Dept of EEE, SITS, Kadapa, AP, India.

<sup>2</sup>Assistant Professor, Dept of EEE, SITS, Kadapa, AP, India.

Corresponding Email: <sup>1\*</sup>madanmadhu212@gmail.com

Received: 17 October 2022    Accepted: 30 December 2022    Published: 01 February 2023

**Abstract:** *The need for power is raising rapidly all across the world right now. This last period has seen a dramatic increase in the severity of global warming brought on by the earth's climate. Greenhouse gas emissions from customary fossil fuel-depend vehicles have risen to the forefront of environmental concerns as the number of cars on the road continues to rise. Pollution from traditional internal combustion engines is rising at an alarming rate. A growing number of people see renewable energy based techniques as ideal answers to the problems of rising fuel efficiency regulations and falling pollution levels. In recent years, interest in hydrogen's potential as a new energy vector has grown rapidly; this is because hydrogen can be converted to electric energy in a fuel cell (FC), making it a viable option for powering fuel cell electric vehicles (FCEV). In comparison to other fuel cell types, the working temperature range of a Proton Exchange Membrane Fuel Cell (PEMFC) makes it the best option for usage in automobiles. As the value of FC modules is rather low, a further action is necessary for interfacing with utility grids in FC-based power sources. Even though a traditional boost converter may increase the DC bus voltage from the FC to the necessary level by the inverter, doing so at a very high duty ratio reduces the converter's efficiency and effectiveness. In this study, we propose using high-gain interleaved DC-DC converters to fix this issue. To provide the electric vehicle's power train, this research introduces a radial basis function network (RBFN) with maximum power point tracking (MPPT) method for PEMFC. To determine the PEMFC's optimum operating point, the planned NN-MPPT method employs a RBFN. FCEVS require dc-dc converters with more switching frequencies and heavy voltage gains for propulsion. A three-phase high voltage-gain interleaved boost converter (HV-GIBC) is also developed for the FCEV method to achieve high voltage-gain. Power semiconductors are stressed by leakage current fluctuation and voltage fluctuations are lessened by the interleaving method. We evaluate the MATLAB/Simulink platform's Fuzzy Logic controller against the RBFN-based MPPT controller in an FCEV system's performance evaluation.*



**Keyword: Fuzzy Logic, RBFN, MPPT, HV-GBIC, FCEV, PEMFC.**

## 1. INTRODUCTION

During the past decade, the political, economic, and scientific sectors have given more thought to the issue of air pollution emissions connected to transportation. Increasing attention is being paid to hydrogen energy-based innovations and fuel cell systems as integral components of the better future of eco-friendly automobiles as a means of reducing reliance on crude oil. These days, automotive scientists spend much of their time creating Transportation that is both cheap and kind on the planet's resources. One of these renewable-energy automobiles, EVs, PHEVs, HEVs and FCEVs are the current market leaders. However, there are a few drawbacks to EVs, PHEVs, & HEVs. I'll start by the Except for quick charging, refuelling an EV or PHEV still takes several hours. Second, electric vehicles' ranges are currently fairly small, and they are especially susceptible to factors like how the driver operates the vehicle, the weather, and whether or not they use any additional equipment. Third, PHEVs and HEVs still use crude oil, thus they can't achieve true zero pollution output. A number of clean energy cars exist, but fuel cell electric vehicles (FCEVs) stand out from the crowd because to their many benefits (quick recharging, extensive range, no pollution emission, etc.). Table 1 displays the results of a worldwide investigation comparing the three businesses' marketed FCEVs. This data clearly shows that PEM fuel cells are the preferred option for these businesses.

Table-1: overall comparison

|               |               | Toyota FCHV-adv                | Toyota Mirai                            | Honda FCX-Clarity | Honda Clarity Fuel Cell | Hyundai Tucson ix35 FCEV        | Hyundai Nexo                    |
|---------------|---------------|--------------------------------|---|-------------------|-------------------------|---------------------------------|---------------------------------|
| Year          |               | 2008                           | 2015                                    | 2008              | 2016                    | 2014                            | 2018                            |
| Vehicle class |               | Sport Utility Vehicle 2WD      | Subcompact car                          | Midsize car       | Midsize car             | Small Sport Utility Vehicle 2WD | Small Sport Utility Vehicle 2WD |
| Fuel cell     | Type          | PEM                            | PEM                                     | PEM               | PEM                     | PEM                             | PEM                             |
|               | Cell quantity | 400 cells (dual line stacking) | 370 cells [1-12] (single line stacking) | --                | --                      | 434 cells (250~450V)            | 440 cells [1-18] (255~450V)     |



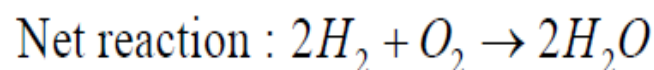
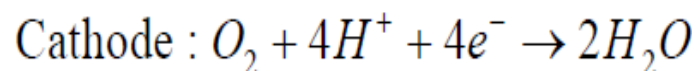
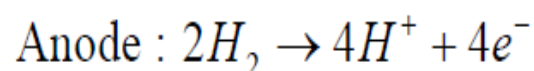
|   |                            |                      |                               |                     |                               |                    |                   |
|---|----------------------------|----------------------|-------------------------------|---------------------|-------------------------------|--------------------|-------------------|
|   | Power density              | 1.4kW/L<br>0.83kW/kg | 3.1kW/L<br>[1-13]<br>2.0kW/kg | 2.0kW/L<br>1.0kW/kg | 3.1kW/L<br>[1-15]<br>2.0kW/kg | 1.65kW/L<br>[1-17] | 3.1kW/L<br>[1-18] |
| Fuel  | Type                       | Hydrogen             | Hydrogen                      | Hydrogen            | Hydrogen                      | Hydrogen           | Hydrogen          |
|   | Storage pressure (nominal) | --                   | 70MPa                         | 35MPa               | 70MPa                         | 70MPa              | 70MPa             |
|   | Storage volume             | 156L                 | 122.4L                        | 171L                | 141L                          | 144L               | 156.6L            |
|   | Fuel storage mass          | --                   | 5.0kg                         | 3.6kg               | 5.0kg                         | 5.64kg             | 6.33kg            |
|   | Refueling time             | --                   | 3 minutes                     | --                  | 3 minutes                     | 3 minutes          | 3 minutes         |
| DC/DC converter for fuel cell                   |                            | No                   | Yes [1-14]                    | No                  | Yes [1-15]                    | No                 | No [1-18]         |
| DC bus voltage                                  |                            | --                   | 650V [1-14]                   | 330V                | 500V [1-15]                   | 400V               | 400V [1-18]       |
| HV battery                                      | Type                       | Ni-MH                | Ni-MH                         | Li-Ion              | Li-Ion                        | Li-Ion             | Li-Ion            |
|   | Voltage                    | 288V                 | 245V                          | 288V                | 358V                          | 180V               | 240V              |
| Motor   | Type                       | AC Synchronous Motor | AC Synchronous Motor          | DC Brushless Motor  | PMSM                          | AC Induction Motor | PMSM              |
|   | Power                      | 90kW-260Nm           | 113kW                         | 100kW               | 130kW                         | 100kW              | 120kW             |
| Driving range (miles)                           |                            | --                   | 312                           | 240                 | 366                           | 265                | 354               |
| Fuel economy: Miles per Kilogram (city/highway) |                            | --/--                | 66/66                         | 60/60               | 68/66                         | 48/50              | 58/53             |



To implement the interleaving approach, converters are wired in parallel. There has been recent exploration on the potential acceptability of IBC in a number of settings. Multi-phase IBC benefits include reduced power fluctuation, reduced switching failure, improved system responsiveness, higher effectiveness, and so on. Adding more interleaved phases improves the system's overall performance. The power fluctuation of the converter may be auxiliary decreased by employing linked inductor. As a result, the conversion network may be made with less space and at a cheap rate. The uses of BLDC motor have undergone great growth in various areas of solar PV system such water pump, electric car since of its more effectiveness, excellent torque-speed features, quiet operation, reduced noise etc. However, a ripple-free input supply is crucial for a motor drive system's performance. If a jittery power source is used to power the motor, the resulting torque ripple will cause the stator phase currents to pulse. When a motor's drive experiences a torque ripple, it results in a fluctuation in speed, as well as vibration and noise. Consequently, the motor's performance suffers. Getting the necessary speed performance from a BLDC motor also requires speed control. In this study, the efficiency of a 3- $\Phi$  IBC with a linked inductor is used to power a BLDC motor that runs on solar energy.

### Fuel Cell

Electrical power may be generated from the chemical energy of a fuel using an FC, which is an electrochemical device. If hydrogen is used as a fuel, electrons and positive hydrogen ions can be extracted at the anode with the use of catalysts. When acting as an oxidant at the cathode, oxygen is drawn from the air. Electrochemical processes include the transfer of electrons from an external load and the exchange of ions across a solid or liquid electrolyte. FC uses an electrochemical mechanism very similar to that of a battery, but they can work indefinitely so long as they have access to fuel and oxygen. Just power, water, and warm are produced by the FC when pure hydrogen is utilised as the fuel. These fundamental chemical changes illustrate the process:



Different types of FCs exist depending on the electrolyte used, including AFC, PAFC, MCFC, SOFC, and PEMFC. The temperature at which they function is an additional criterion for categorising FCs. PEMFC is superior to other FCs in terms of power density, weight, and size. Table 2 summarises the various FCs' distinguishing features.

Table-2: Fuel cells characteristics

| Fuel cell type           | Electrolyte                                      | Operating temperature | Advantages  | Disadvantages  |
|--------------------------|--|-----------------------|---|--|
| Alkaline                 | Potassium hydroxide or alkaline polymer membrane | <100°C                | -Low temperature<br>-Lower cost components  | -Sensitive to CO <sup>2</sup> in fuel<br>-Electrolyte management |
| Phosphoric acid          | Phosphoric acid                                  | 150°–200°C            | -Increased tolerance to fuel impurities   | -Expensive catalysts<br>-Sulfur sensitivity                      |
| Molten carbonated        | Lithium potassium carbonate salt                 | 600°–700°C            | -High efficiency<br>-Fuel flexibility   | -High temperature<br>-Low power density                          |
| Solid oxide              | Ytria stabilized zirconia                        | 500°–1,000°C          | -High efficiency<br>-Fuel flexibility   | -High temperature<br>-Limited number of shutdowns                |
| Proton exchange membrane | Solid polymer                                    | <120°C                | -Low temperature<br>-Solid electrolyte (reduces corrosion, electrolyte management problems) | -Expensive catalysts<br>-Sensitive to fuel impurities            |

Single FC, as seen in Figure 1(a), which is impractically low. To get a greater output voltage, many cells must be linked in series, leading in an FC stack, as illustrated in Fig 1(b).

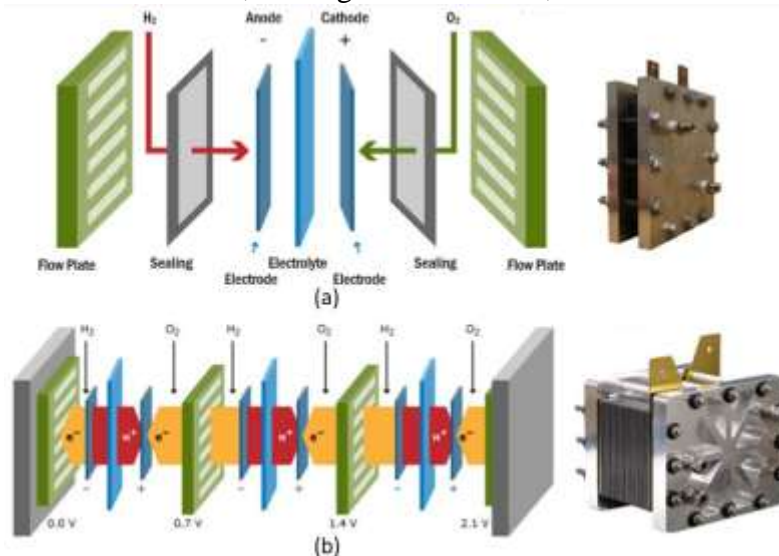


Fig.1: structure of fuel cell. (a) Single cell (b) FC stack.

### System Modelling

The electric motor, which provides propulsion for the vehicle, receives its power from the inverter that is powered by the output voltage of the suggested technique. A key component of FCEVs is the electric motor. The size and cost of the fuel cell may be drastically cut down with a good motor. Most manufacturers have hitherto relied on DC motors for EV applications. However, DC motors are unreliable and require frequent servicing as of their brushes and other moving parts. As of now, FCEV applications favour the use of PMBLDC motors because of their easy operation, dependability, and durability. BLDC motor powered FCEV system with three-phase HV-GIBC is depicted in Fig.2. This unit is made up of a BLDC motor, VSI, three-phase HV-GIBC, and a 1.26 kW PEMFC. The 3- $\Phi$  IBC acts as a connection point for PEMFC and VSI. In order to get the most juice out of the fuel cell, an MPPT algorithm based on a recurrent back-feeding feedforward network has been developed. The BLDC motor receives power from the three-phase IBC, which is converted into VSI for delivery to the motor. The electrical synchronization of the BLDC motor is used to operate the VSI's switches. The shaft of the motor is coupled to the wheels of the vehicle to provide forward motion.

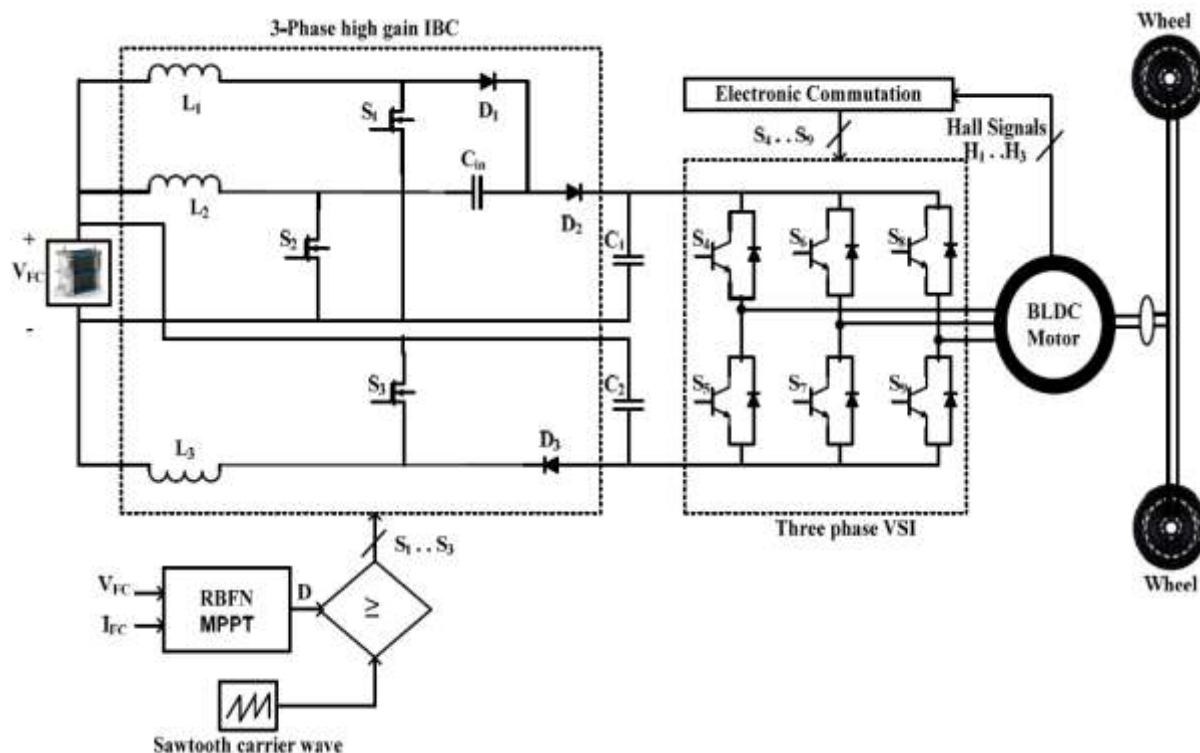


Fig.2: Proposed configuration of FCEV.

Switches ( $S_1$ ,  $S_2$ , and  $S_3$ ) plus diodes create up the suggested device ( $D_1$ ,  $D_2$  and  $D_3$ ). The inductors  $L_1$ ,  $L_2$ , and  $L_3$  are used as filters in phases 1, 2, and 3. The voltage input  $V_{FC}$ , the voltage output  $V_O$ , & the load resistance  $R$  are all shown in the equation. These presumptions guide our examination of the proposed HV-GIBC: let's suppose that in all three phases, the inductors are perfect: ( $L_1 D L_2 D L_3 D L$ ). The capacitors  $C_1$  and  $C_2$  used for filtering are

interchangeable (C1 D C2 D C). Continuous Conduction Mode is always in effect while using the suggested converter (CCM). It is expected that the power waves across the capacitor & inductor are minimal.

The fuel cell technology requires MPPT so that the most possible power may be drawn from it under varying environmental circumstances. A RBFN-based MPPT controller is constructed for the optional setup, and its performance is evaluated in comparison to that of FLC. As a feedforward neural network model, RBFN may be trained in both supervised and unsupervised ways. As can be seen in Fig.3, an RBFN normally has three layers: an input layer, a concealed structure, and an output structure. While the linear output structure, the hidden structure uses a non-linear RBFN.

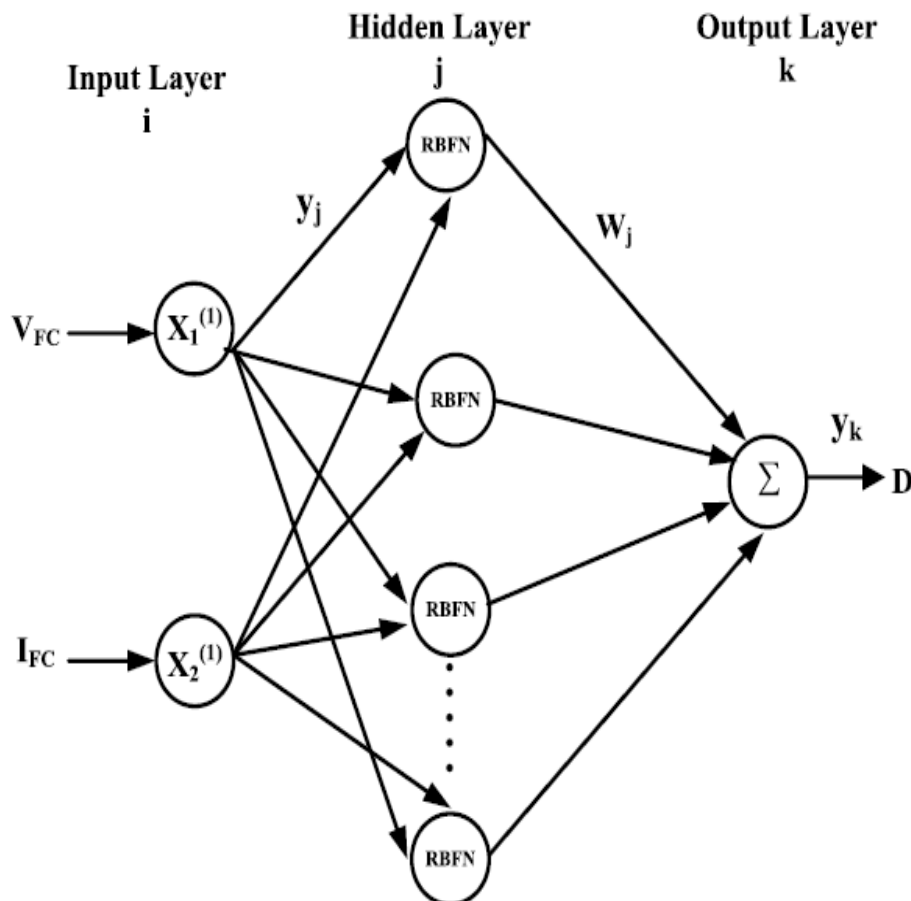


Fig.3: structure of RBFN.

## 2. SIMULATION RESULTS

Using the MATLAB/Simulink environment, we examine the effectiveness of the suggested FCEV system driven by BLDC motors.

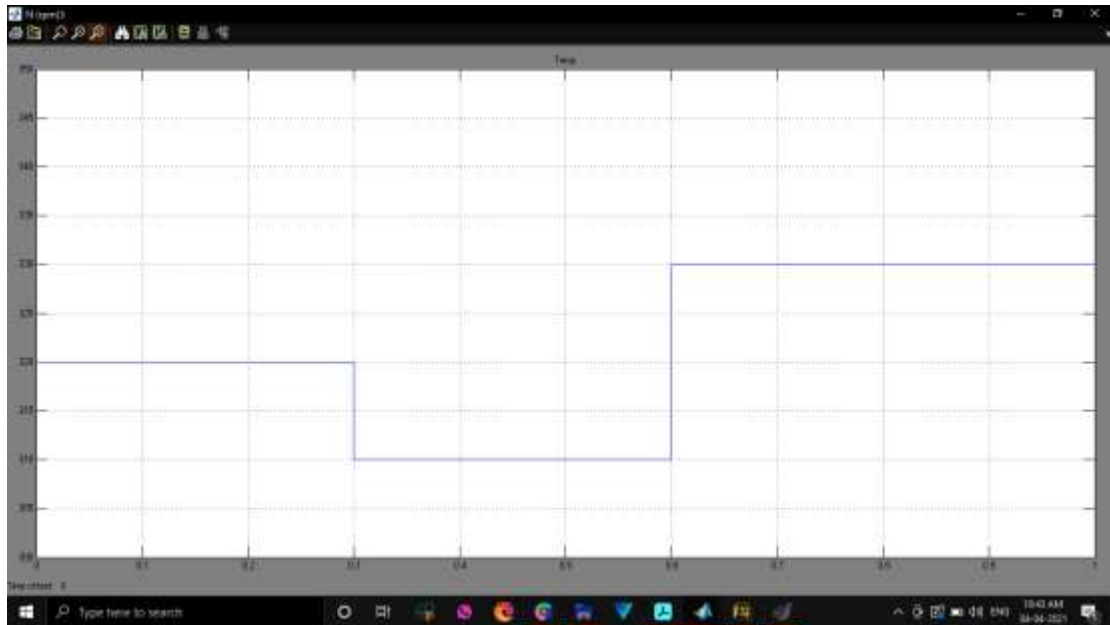
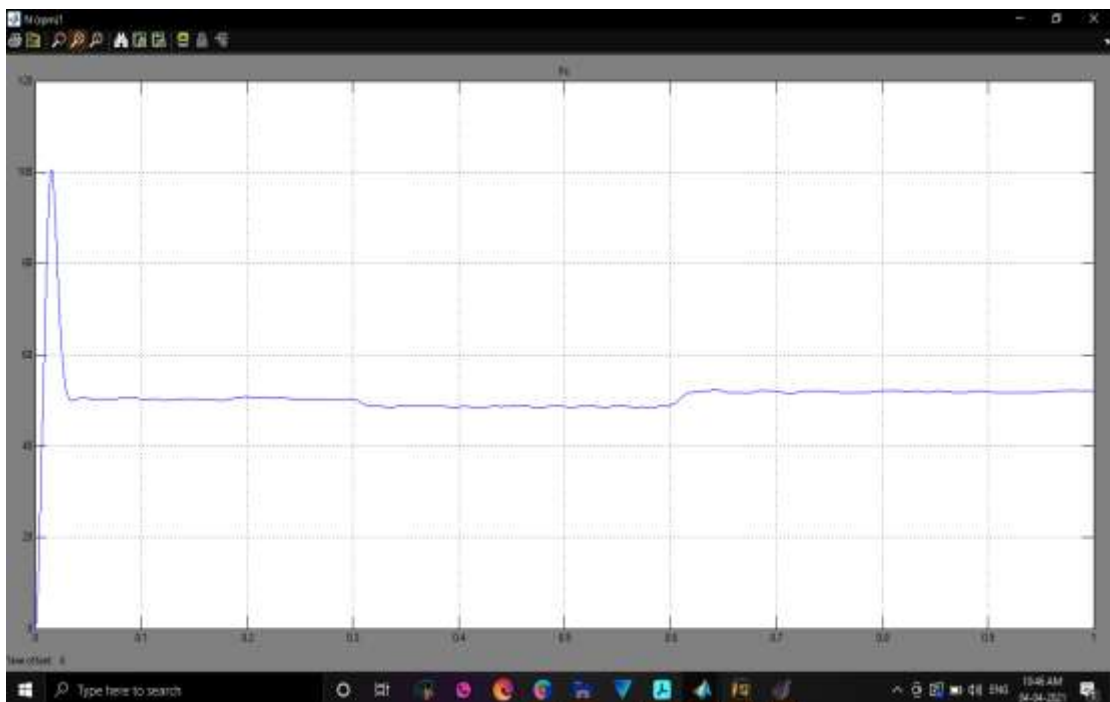


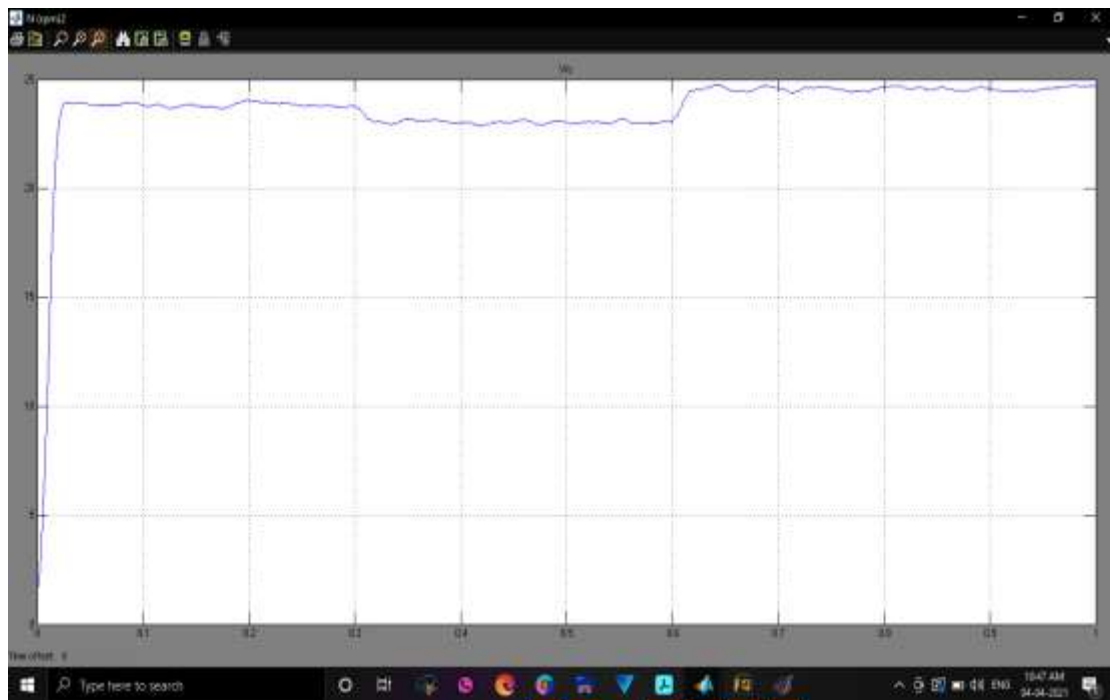
Fig.4: Temperature changes in PEMFC system.

The following scenarios involving significant variations in fuel cell temperature are examined in the analysis of the FCEV system's dynamic response: As can be seen in Fig. 4, the temperature ranges from 0 to 0.3 seconds at  $T = 320^0\text{K}$ , from 0.3 seconds to 0.6 seconds at  $T = 310^0\text{K}$ , and from 0.6 seconds to 0.9 seconds at  $T = 330^0\text{K}$ .

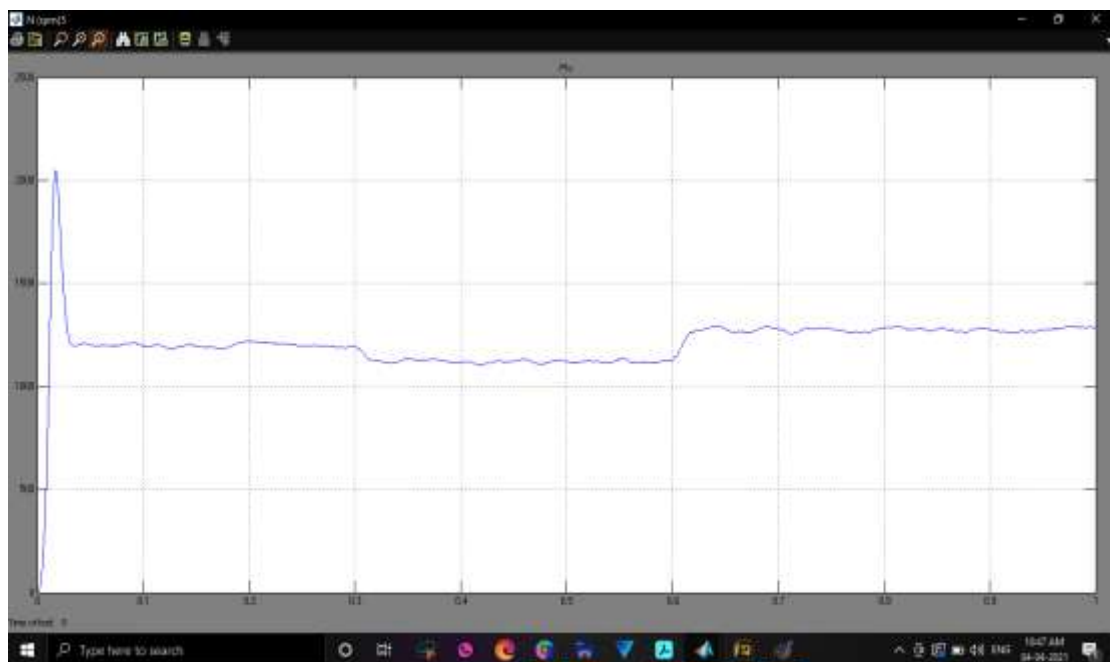


$I_{fc}$





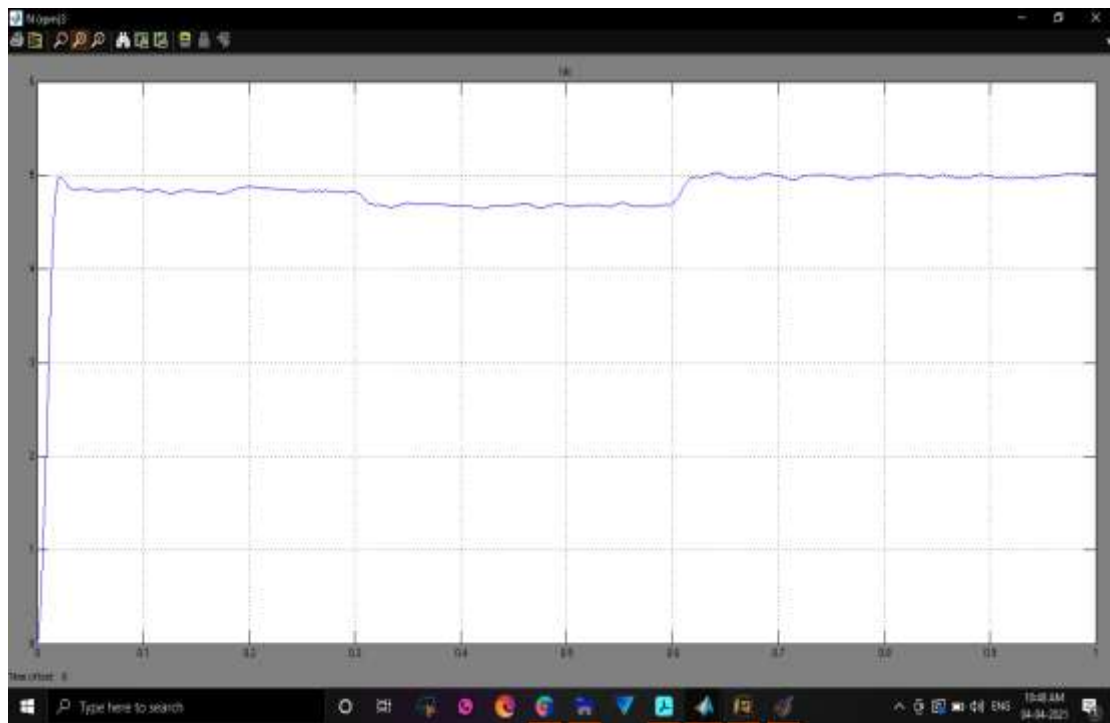
V<sub>fc</sub>



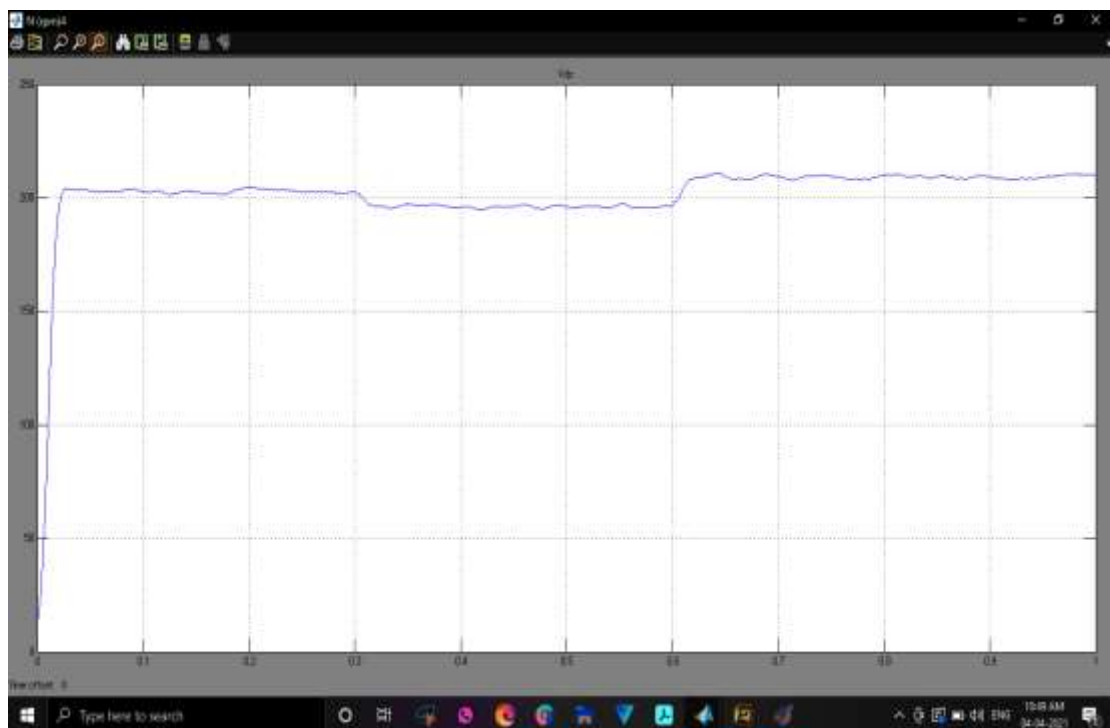
P<sub>fc</sub>

Fig.5: Fuel cell output current, voltage and power at different temperatures.

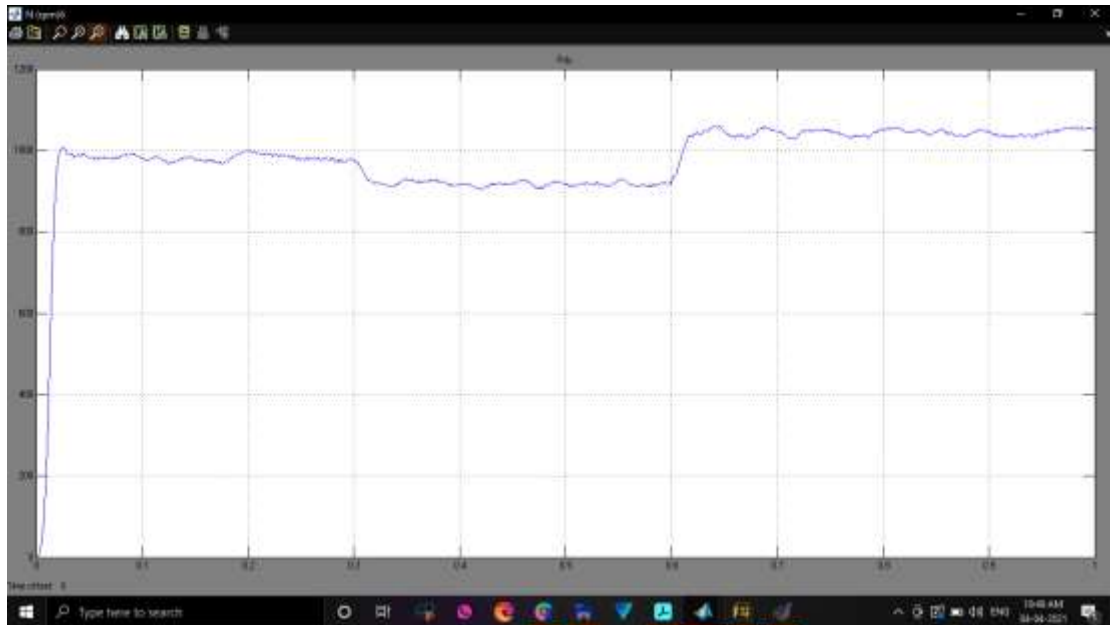
Fig. 5 depicts the fuel cell's output current, voltage, and power waveforms at various temperatures. The fuel cell produces 1080W from zero to thirty seconds, 970W from thirty seconds to sixty seconds, and 1220W from sixty seconds to ninety seconds.



Idc



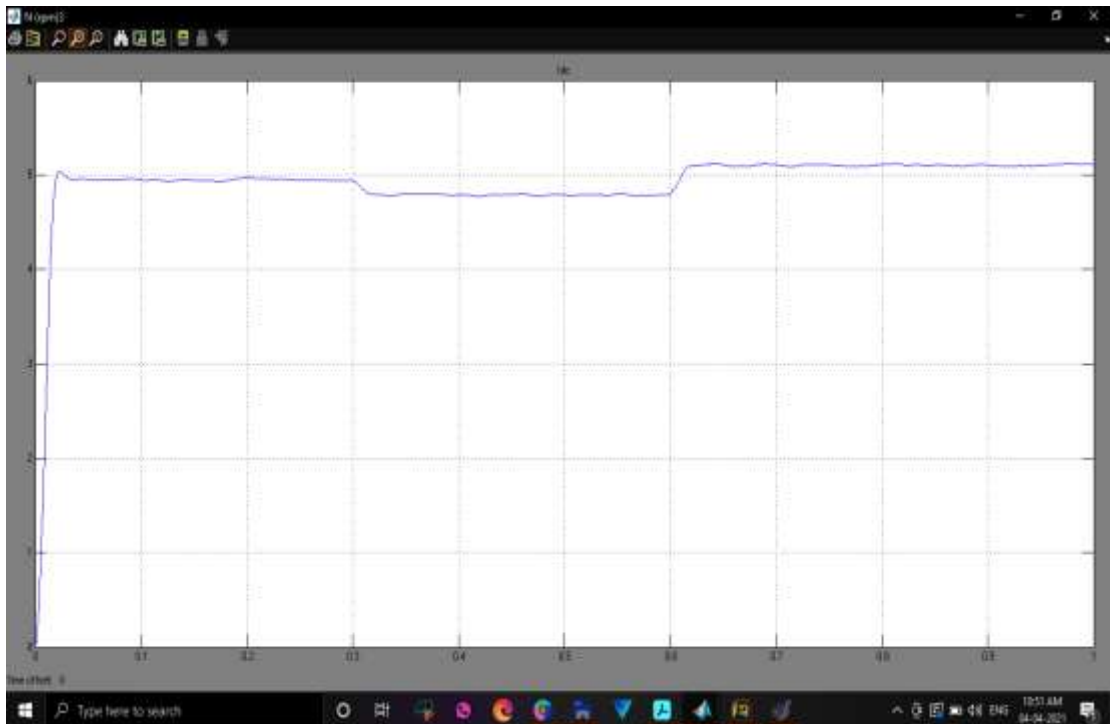
Vdc



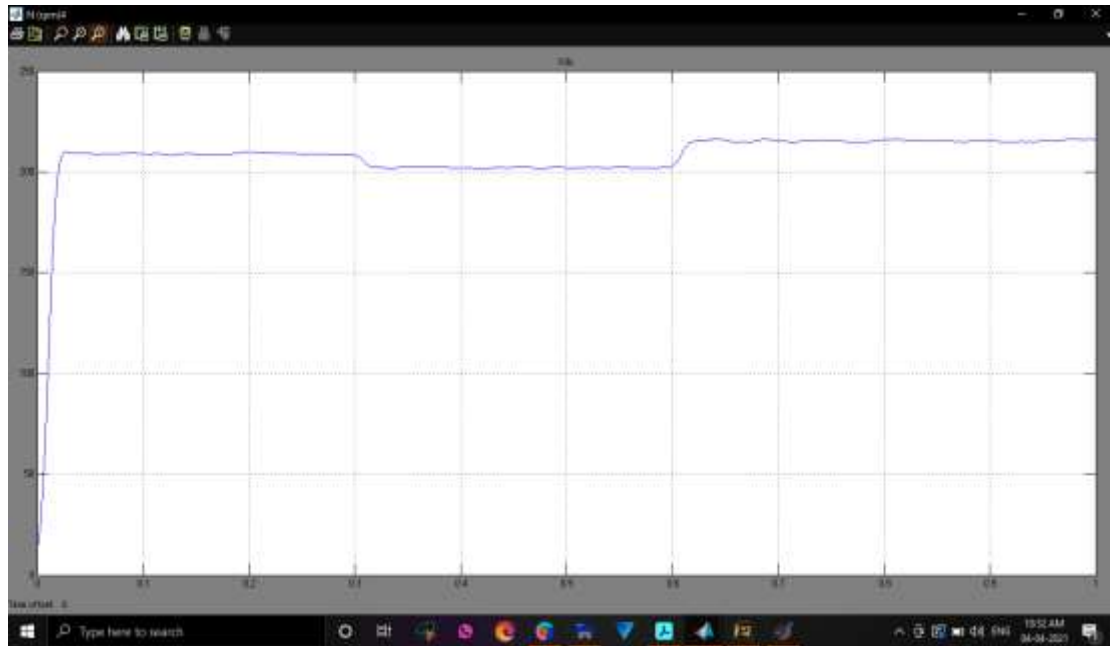
P<sub>dc</sub>

Fig.6: DC link output current, voltage and power at different temperatures using FLC.

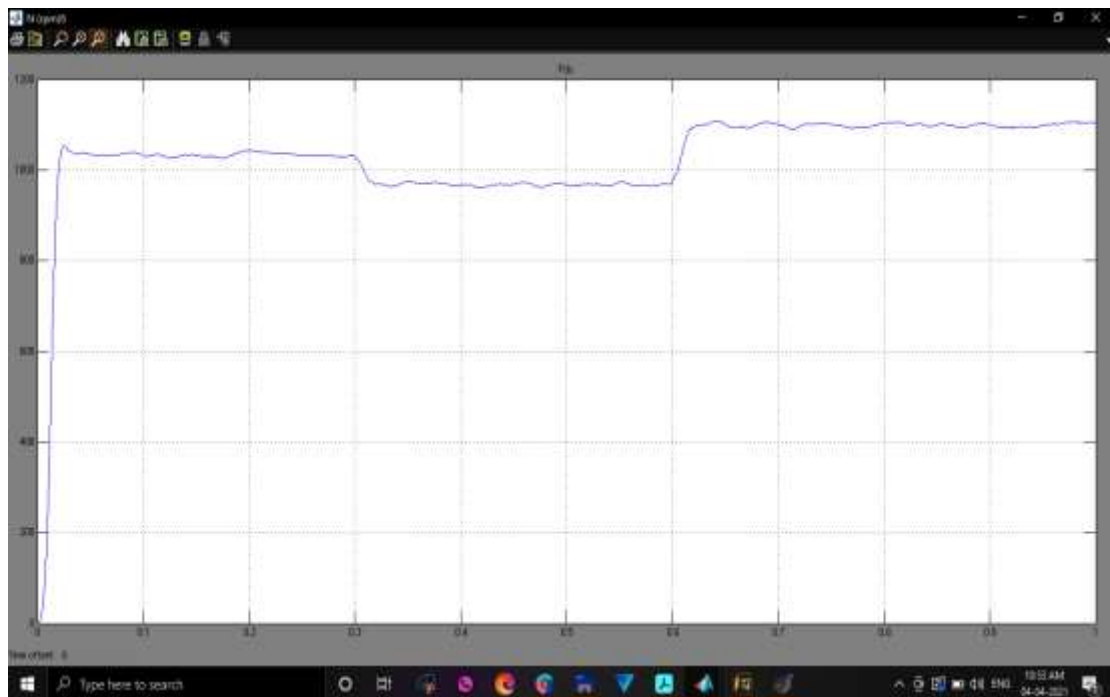
Current, voltage, and power in the DC connection measured using the FLC-based MPPT method is displayed in Fig. 6. At 320<sup>0</sup>K, it produces 1000W, at 310<sup>0</sup>K, it produces 830W, and at 330<sup>0</sup>K it produces 1150W of power.



I<sub>dc</sub>



Vdc



Pdc

Fig.7: DC link output current, voltage and power at different temperatures using RBFN.

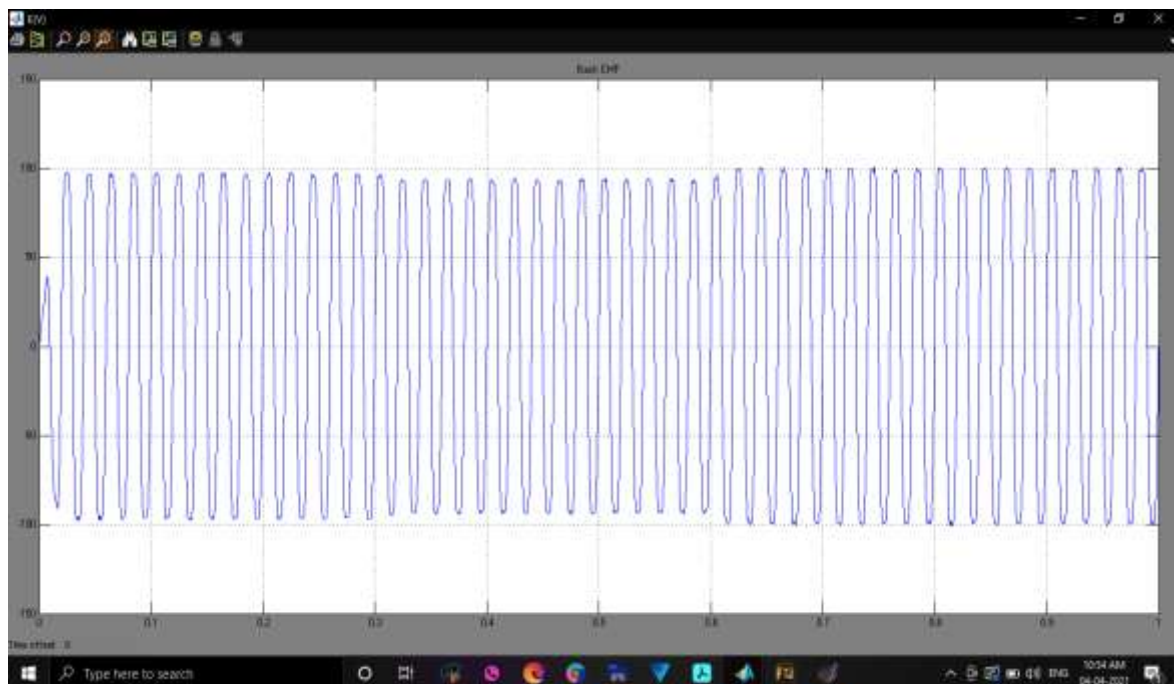
In Fig.7, we see the DC link's current, voltage, and power after being processed by the suggested RBFN-based MPPT controller. The suggested controller supplies 1050W at 320<sup>0</sup>K, 900W at 310<sup>0</sup>K, and 1200W at 330<sup>0</sup>K.



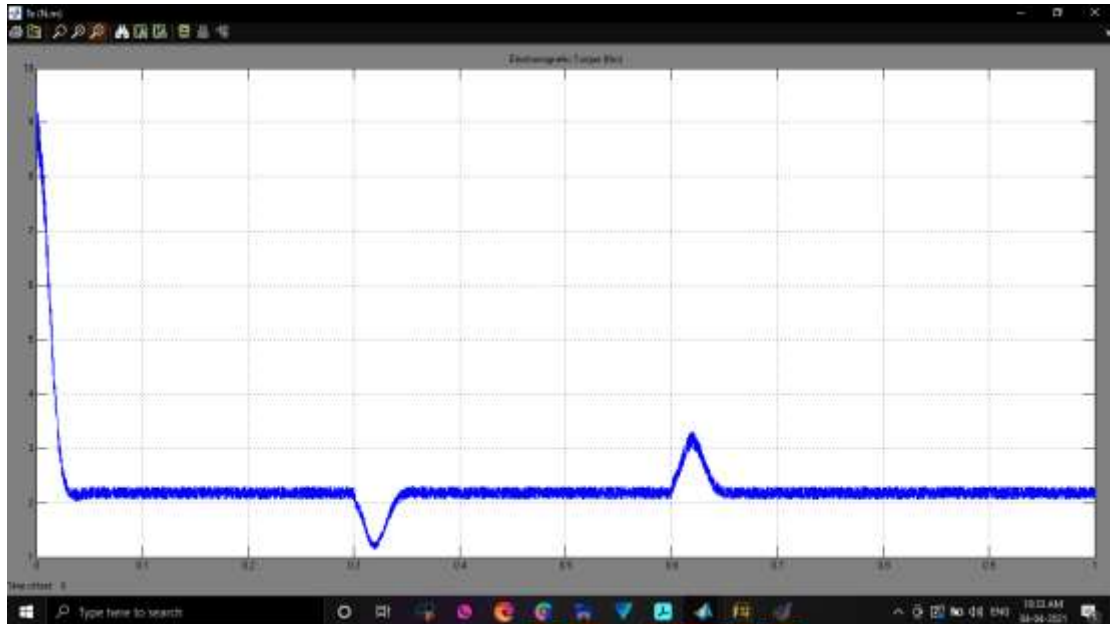
Pdc

Fig.8: Comparison of DC link power with both RBFN and Fuzzy based MPPT controllers.

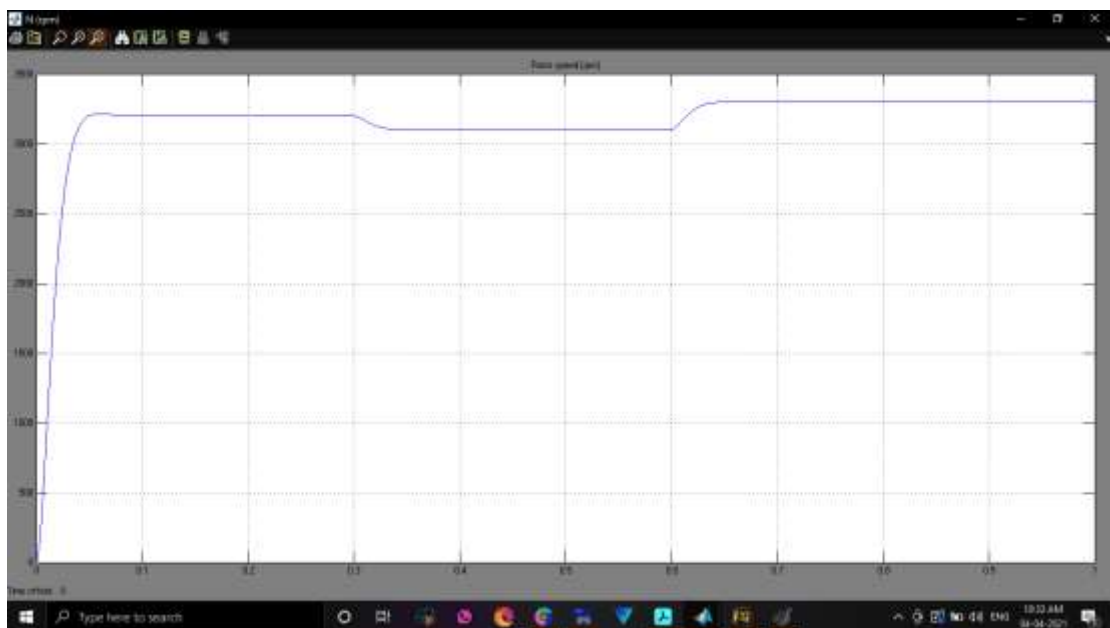
Figure 8 shows a comparison between the RBFN-based MPPT controller and the fuzzy logic-based MPPT controller when applied to a fuel cell. As can be shown in Fig. 8, the DC link power produced by the suggested controller is significantly higher than that generated by the FLC.



Back EMF(E)



$T_e$



Speed(N)

Fig.9: BLDC motor parameters.

In Fig.9, we see the BLDC motor's initial and sustained performances across a range of FC temperatures. Variables of the motor, including stator current ( $I_{sa}$ ), back electromotive force (E), electromagnetic torque ( $T_e$ ), and load torque (TL), are shown at varying fuel-cell temperatures. From zero to 0.3 seconds, the BLDC motor spins at 3300 rpm; from 0.3 to 0.6



seconds, it spins at 2400 rpm; and from 0.6 to 0.9 seconds, it spins at 3700 rpm. Even when the speed changes, the BLDC motor's torque stays the same.

### **3. CONCLUSION**

In modern FCEVs, increasing the PEMFC output voltage to an appropriate level necessitates the use of a DC/DC converter. The primary focus of this thesis is on developing a DC/DC boost converter that meets these requirements by virtue of its high efficiency, small size, and high voltage gain ratio. As a result of the interleaved design, the ripple in the FC current is reduced, and the duration of the FCs is lengthened. Multi-phase operation allows the large input current to be distributed evenly across the system. Because of this, the electrical load on the power switch is reduced, and the converter's dependability and redundancy are both improved. The results of the simulations show that the RBFN based MPPT controller is more effective than the fuzzy logic controller in locating the maximum power point. Electromagnetic torque, speed, and back EMF are also examined, along with other BLDC motor evaluation criteria, across a range of FC system temperatures.

### **4. REFERENCES**

1. C. C. Hua, Y. H. Fang and C. J. Wong, "Improved solar system with maximum power point tracking", *IET Renewable Power Generation*, vol. 12, no. 7, pp. 806-814, May 2018.
2. O. Ezinwanne, F. Zhongwen and L. Zhijun, "Energy performance and cost comparison of MPPT techniques for photovoltaics and other applications", *Energy Procedia* (Elsevier), vol. 107, pp. 297-303, February 2017.
3. P. K. Vineeth Kumar and K. Manjunath, "A comparative analysis of MPPT algorithms for solar photovoltaic systems to improve the tracking accuracy", *International Conference on Control, Power, Communication and Computing Technologies (ICCPCCT)*, IEEE conference, pp. 540-547, Kannur, India, March 2018.
4. Balavenkata Muni, N., Sasikumar, S., Hussain, K., Reddy, K.M. (2022). A Progressive Approach of Designing and Analysis of Solar and Wind Stations Integrated with the Grid Connected Systems. In: Kalinathan, L., R., P., Kanmani, M., S., M. (eds) *Computational Intelligence in Data Science. ICCIDS 2022. IFIP Advances in Information and Communication Technology*, vol 654. Springer, Cham. [https://doi.org/10.1007/978-3-031-16364-7\\_7](https://doi.org/10.1007/978-3-031-16364-7_7)
5. K.MEENENDRANATH REDDY, & SYED RESHMA. (2022). A Comparative Analysis of Integrated DC Microgrid with Hybrid Power Generation Systems by an Intelligent Control Strategy. *International Journal of Recent Research in Electrical and Electronics Engineering*, 9(2), 1–10. <https://doi.org/10.5281/zenodo.6538769>
6. M. Z. Hossain, N. A. Rahim and J. a. Selvaraja, "Recent progress and development on power DC-DC converter topology, control, design and applications: A review", *Renewable and Sustainable Energy Reviews*, (Elsevier) vol. 81, part 1, pp. 205-230, January 2018.



7. S. J. Chen, S. P. Yang, C. M. Huang and C. K. Lin, “Interleaved high step-up DC-DC converter with parallel-input series-output configuration and voltage multiplier module”, IEEE International Conference on Industrial Technology (ICIT), pp. 119-124, Toronto, Canada, March 2017.
8. Sharabu. Siddhartha Achari, Galigeri. Aravindakumar, Ketha. Govardhan and K.Meenendranath Reddy. Wireless Electrical Power Transmission Using Spark Gap Tesla Coil (SGTC). International Journal for Modern Trends in Science and Technology 2022, 8(07), pp. 38-50. <https://doi.org/10.46501/IJMTST0807007>
9. K.Meenendranath Reddy, G.Hussain Basha, Saggi Raj Kumar, V.Srikanth. An Efficient MPPT Technique using Fuzzy/P&O Controller for PV Applications. International Journal for Modern Trends in Science and Technology 2021, 7, pp. 106-111. <https://doi.org/10.46501/IJMTST0710017>
10. M. Shaneh, M. Niroomand and E. Adib, “Ultra high-step up non-isolated interleaved boost converter”, IEEE Journal of Emerging and Selected Topics in Power Electronics, Early Access, December 2018.
11. A. Naderi and K. Abbaszadeh, “High step-up DC–DC converter with input current ripple cancellation”, IET Power Electronics, vol. 9, no. 12, pp. 1755-4535, May 2016.
12. Dr. P.Sankar Babu, K.Meenendranath Reddy and S.Sneha Madhuri. Improvement of Power Quality in Renewable Energy Integrated Microgrid System Using CMBC. International Journal for Modern Trends in Science and Technology 2021, 7 pp. 299-303. <https://doi.org/10.46501/IJMTST0712058>
13. Kavitha, K., K. Meenendranath Reddy, and Dr. P.Sankar Babu. 2022. “An Improvement of Power Control Method in Microgrid Based PV-Wind Integration of Renewable Energy Sources”. Journal of Energy Engineering and Thermodynamics(JEET) ISSN 2815-0945 2 (06):18-28.
14. M. Lasheen, A. K. A. Rahman, M. A. Salam and S. Ookawara, “Adaptive reference voltage-based MPPT technique for PV applications”, IET Renewable Power Generation, vol. 11, no. 5, pp. 715-722, January 2017.
15. P. Naga Sai Charan, & K. Meenendranath Reddy. (2023). An Analysis of Multilevel Converter for Faster Current Control in a DC Microgrid with Extremely Low-Impedance Interconnections. Journal of Image Processing and Intelligent Remote Sensing(JIPIRS) ISSN 2815-0953, 3(01), 18–29. <https://doi.org/10.55529/jipirs.31.18.29>.
16. B. Akhlaghi and H. Farzanehfard, “Family of ZVT Interleaved Converters With Low Number of Components”, IEEE Transactions on Industrial Electronics, vol 65, no. 11, pp. 8565-8573, November 2018.
17. S. Banerjee, A. Ghosh and N. Rana, “An improved interleaved boost converter with PSO-based optimal type-III controller”, IEEE Journal of Emerging and Selected Topics in Power Electronics, vol. 5, no. 1, pp. 323-337, March 2017.